# Liver Blood Flow: Non-Invasive Estimation Using a Gamma Camera

W B Tindale, D C Barber, H L Smart and D R Triger

*Proceedings of the Institution of Mechanical Engineers, Part H: Journal of Engineering in Medicine* 1992 206: 99
DOI: 10.1243/PIME_PROC_1992_206_273_02

# Liver blood flow: non-invasive estimation using a gamma camera

**W B Tindale,** MSc, PhD, MIPSM, **D C Barber,** BA, MSc, PhD, FIPSM,
**H L Smart,** MB, BS, DM, MRCP and **D R Triger,** BM, BCh, MA, DPhil, FRCP
Departments of Medical Physics and Medicine, Royal Hallamshire Hospital, Sheffield

*A non-invasive radioisotope technique for the measurement of total liver blood flow (TBF) is described. The method requires the use of two intravenously administered tracers, $^{99m}Tc$ (technetium 99m) human serum albumin (HSA) and $^{99m}Tc$ colloid. Computer analysis of first-pass time activity curves for HSA for liver and lung tissues yields values for the arterial and portal contributions to liver blood flow, from which TBF can be determined. These values are then corrected for attenuation using the images of the colloid distribution. The use of the method is illustrated in 17 subjects. Assumptions, limitations and possible applications of the technique are discussed.*

## 1 INTRODUCTION

The measurement of liver blood flow is an important aspect of any study of liver physiology and the changes that occur in disease. The most commonly used technique for its measurement is the indirect Fick method, which has been widely documented (**1**, **2**). However, since this necessitates hepatic vein catheterization, it is clearly not without risk to the patient. Metered flow probes have also been employed in specific situations to study liver blood flow (**3**), but the invasive nature of the procedure makes it unsuitable for routine use.

Non-invasive techniques for measuring total or partial flow have included the use of drugs which are fully absorbed by the gut and eliminated solely by the liver (**4**) and pulsed Doppler measurements for the estimation of portal blood flow (**5**). The radioisotope methods that have been employed have largely concentrated on the measurement of effective or functional blood flow by clearance techniques (**6**). However, as noted by Groszman (**7**), changes in clearance due to variation in flow cannot be distinguished from those due to cellular dysfunction unless the extraction efficiency of the liver for the particular radiopharmaceutical is known. In general this is not known, although methods have been suggested for its determination (**8**), and it is likely to vary with disease state (**9**).

For obvious reasons an intravascular non-extracted tracer cannot be used to measure blood flow by clearance. However, this paper will show that such a tracer can be used, with appropriate data analysis, to provide a measure of total blood flow to the liver.

## 2 THEORY

Delivery of a non-extracted non-diffusible tracer to the liver is dependent on both hepatic arterial and portal venous flow. An intravenous bolus of activity will reach the liver first by the arterial route and later by the portal venous route. The extent of this temporal separation in tracer arrival is governed by its transit time in the splenic and mesenteric circulations. Since the tracer is not extracted, the final level of activity in the organ after complete mixing is dependent on its blood volume.

A generalized method for calculating absolute organ blood flow, based on the analysis of first-pass time activity curves of an intravascular tracer, has recently been described by Peters *et al.* (**10**). The method is based on the microsphere technique in which, following left ventricular injection, radiolabelled microspheres, which are extracted with 100 per cent efficiency, become trapped in each distinct vascular bed within the body in proportion to the fraction of cardiac output supplied to that bed. The fraction of cardiac output delivered to a given organ can therefore be determined from the ratio of the final height of the organ time activity curve (TAC), after correction for attenuation, and the injected dose. Furthermore, since the transit time of such a tracer through an organ can be considered to be infinite, the TAC will have a shape (but not magnitude) that is identical to the integral of the first-pass TAC recorded over any major artery. In this ideal case no recirculation occurs. When the organ transit time is finite, as for an intravascular tracer, the integrated arterial curve can be used to predict the shape the organ TAC would take if the tracer behaved like microspheres, providing an appropriate scaling factor can be determined and a correction made to the arterial curve for recirculation. For the latter, previous authors (**10**) have employed a gamma function curve-fitting procedure.

Peters *et al.* (**10**) use the ratio of the maximum upslopes of the arterial and organ TACs to calculate the scaling factor. This can lead to errors both in the presence of noisy data and if significant output occurs from the organ before the time of maximum input. For an organ such as the liver with a dual blood supply, additional errors will be introduced if portal inflow of tracer occurs before the time of maximum arterial input. An alternative approach is to calculate the scaling factor using a model of the liver impulse retention function (IRF) from which best-fit hepatic arterial and portal venous signals can be determined as separate components. This method, which is discussed in detail elsewhere (**11**), is likely to be less dependent on noise since all of the data from the first-pass liver TAC are used in the analysis. It is assumed that there is a temporal

*The MS was received on 16 December 1991 and was accepted for publication on 6 August 1992.*


0954-4119/92 $3.00 + .05

separation between tracer arrival via the hepatic artery and tracer arrival via the portal vein and that the liver is homogeneous throughout with respect to the two components of flow.

The liver impulse retention function (IRF) can be obtained by a constrained deconvolution technique (**11**). While other techniques have employed deconvolution in the study of liver blood flow (**12**), this method differs in approach in that it uses a simple model of the IRF as a starting point for the analysis. The parameters of the model are adjusted until the liver curve generated by convolving the model IRF with the arterial curve best fits (in a least-squares sense) the measured liver curve. The model contains two explicit components, one for the hepatic arterial component of flow and one for the portal component; the hepatic arterial flow fraction may be estimated from the height of these two components. Convolution of each of the components of the IRF with the arterial curve (taken from the image sequence of either the heart or lung) generates a hepatic arterial TAC and a portal TAC which may be summed to give a theoretical liver curve. It should be noted that this technique does not require a gamma function fit to the arterial curve as a correction for recirculation since this is implicit in the deconvolution process.

The height $h$ of the hepatic arterial component of the IRF represents the scaling factor between the integrated blood concentration curve and the hepatic artery signal. Thus, the integrated blood concentration curve, when scaled by this factor and corrected for recirculation, yields a TAC which represents what the liver curve would look like if the tracer behaved in a manner identical to microspheres and there was no portal flow. The fraction of cardiac output (CO) passing along the hepatic artery is given by

$$\frac{\mathrm{ABF}}{\mathrm{CO}} = h\frac{\int B(t)\,\mathrm{d}t \times C_{\mathrm{B}}}{D \times S} \tag{1}$$

where ABF is the artery blood flow, $B(t)$ is the recirculation corrected blood curve, $D$ is the injected dose, $S$ is the detector sensitivity (counts/s MBq) and $C_{\mathrm{B}}$ is an attenuation correction factor for the liver for the projection employed. As noted by Peters *et al.* (**10**), for an intravascular tracer, CO is given by

$$\mathrm{CO} = \frac{D \times S}{\int B(t)\,\mathrm{d}t \times C_{\mathrm{c}}} \tag{2}$$

where $C_{\mathrm{c}}$ is a calibration factor that converts the amplitude of the blood concentration curve to units of cps/ml. In the derivation of equation (2), a spike injection (delta function) of tracer into the heart, with instantaneous mixing in the ventricle, is assumed.

Combining equations (1) and (2) yields the hepatic artery flow in millilitres per second as

$$\mathrm{ABF} = h\frac{C_{\mathrm{B}}}{C_{\mathrm{c}}} \tag{3}$$

The ratio of $h$ to the sum of the heights of the two components of the IRF $(h + p)$ represents the arterial–total blood flow ratio. Total liver blood flow can therefore be expressed as

$$\mathrm{TBF} = (h + p)\frac{C_{\mathrm{B}}}{C_{\mathrm{c}}} \tag{4}$$

The calibration factor $C_{\mathrm{c}}$ can be determined simply by relating the count rate from a venous blood sample taken at any time $t$ after equilibration of the tracer to the count rate at time $t$, $H(t)$, over the region (heart or lung) used to define the shape of the blood concentration curve. Thus, for a blood sample of volume $V$ with a count rate $T$,

$$C_{\mathrm{c}} = \frac{H(t) \times V}{T} \tag{5}$$

The attenuation correction factor $C_{\mathrm{B}}$ is the ratio of the total activity in the liver to the count rate from the liver for the particular view employed. The theoretical basis for the calculation of total activity relies on the assumption of negligible activity in the tissues overlying the organ. The distribution of an intravascular tracer is such that it does not allow this assumption to be satisfied. A second study, employing colloid (which is accumulated and retained by the liver with minimal background contribution) as the tracer, is therefore required for the calculation of $C_{\mathrm{B}}$.

## 3 METHODS

A total of 15 subjects under investigation for suspected liver disease were studied. These comprised eight cirrhotic and seven non-cirrhotic patients, classified on the basis of liver biopsy. Four of the seven non-cirrhotic patients had evidence of alcoholic liver injury, showing fat with or without minor fibrosis. Two additional volunteer subjects, with no history of liver disease, were also investigated. All subjects were starved from midnight on the night preceding the test. In the morning, an intravenous injection of 75 MBq $^{99\mathrm{m}}$Tc (technetium 99m) tin colloid was given, which was followed after 15 minutes by a standard liver scan obtained using an Elscint large-field-of-view gamma camera, interfaced to a Research Machines Nimbus microcomputer. All studies were carried out using a low-energy, general-purpose parallel hole collimator. The right lateral view was acquired with cobalt-57 markers on the anterior and posterior skin surfaces in order to outline the body contour. The image sequence was terminated with an anterior view with the patient in the supine position. Without moving the patient a 5 ml venous blood sample was withdrawn from an arm vein into a preweighed vial so that the residual vascular concentration of tracer could be estimated. This was followed by a fast bolus intravenous injection of 400 MBq $^{99\mathrm{m}}$Tc human serum albumin (HSA) into the antecubital fossa of the opposite arm, with dynamic imaging over the chest and upper abdomen for 10 minutes. The image sequence comprised 60 images each of 1 second duration followed by 27 images each of 20 seconds duration. The injection of $^{99\mathrm{m}}$Tc HSA was delivered between 10 and 20 seconds after the start of data acquisition. The images obtained before injection provided a background baseline of the colloid distribution and were subsequently used for data subtraction. During acquisi-

tion of the final image a 5 ml venous blood sample was withdrawn into a preweighed vial. Both blood samples were weighed and counted separately using the gamma camera.

## 4 DATA ANALYSIS

### 4.1 Time activity curve generation

The time activity curves representing tracer activity in the liver and in the arterial blood supplying the liver must be obtained free of contamination or cross-talk from other structures. This is usually attempted by careful selection of the position and size of the region used to generate the TAC. However, choice of the correct region is not always obvious and a small region only samples part of the organ, which may not be typical. An alternative approach to generating TACs that takes cross-talk into account is factor analysis. This has the advantage of allowing a larger portion of the liver to be analysed than would be possible with simple region-of-interest analysis, thus minimizing any error that may result from vascular inhomogeneities. For this reason, in this study TACs were obtained by a factor analysis technique (**13**). However, since the subsequent analysis is equally applicable to curves obtained by region-of-interest analysis, details of our curve extraction technique will not be given here. The right lung TAC was taken as being the best estimate of the blood concentration curve.

### 4.2 Determination of $C_B$

The attenuation correction factor $C_B$ was calculated using a modification of a method described by Fleming (**14**). He showed that for a rod of activity of length $D$ in the body, with uniform activity $A$ MBq/ml and unit cross-sectional area, the total activity can be expressed as

$$AD = \frac{(R_A R_p)^{1/2}}{\{(\sinh(\mu D/2))/(\mu D/2)\} \exp(-\mu L/2) S} \quad (6)$$

where $R_A$ and $R_p$ are the count rates obtained in the anterior and posterior projections, $S$ is the detector sensitivity, $L$ is the body thickness and $\mu$ is the linear attenuation coefficient for the rod and the surrounding tissues (assumed equal). The count rate in the anterior projection is given by

$$R_A = \frac{SA}{\mu} \exp(-\mu d)\{1 - \exp(-\mu D)\} \quad (7)$$

where $d$ is the thickness of the tissue overlying the rod. Under conditions in which background activity in the overlying tissues is negligible, equation (7) applies at each point in the anterior image of the colloid distribution in the liver. If it can be assumed that $d$ is constant for all points, then for a uniform distribution of tracer $R_A/\{1 - \exp(-\mu D)\}$ is a constant whose value can be determined from the maximum pixel count rate, $R_{A,\max}$, and the maximum liver dimension, $D_{\max}$, on the right lateral view. The value of $D$ at all other points can then be determined by substituting the individual pixel count rates into equation (7).

The corresponding activity at each point is given by equation (6) with substitution of the appropriate value of $D$. The correction factor $C_B$ then becomes

$$C_B = \frac{\sum AD \times S}{\sum R_A} \quad (8)$$

The maximum abdominal thickness at the level of the liver was determined from the average distance between the anterior and posterior skin surface markers on the right lateral view of the colloid study. The value of $L$ was obtained by scaling this result by a factor of 0.89 (**14**). The maximum liver dimension in the right lateral projection, $D_{\max}$, was calculated automatically from a contour generated around the liver, corresponding to 12 per cent of the maximum pixel count rate. The contour level was selected on the basis of results from liver phantom studies, which showed good agreement between calculated and actual liver activities when this level was selected. Alignment of the anterior and posterior images, necessary for the generation of the geometric mean image, $(R_A R_p)^{1/2}$, was achieved by creating a 12 per cent contour around the anterior image of the liver and visually aligning the mirror image of the posterior view with this. A measured linear attenuation coefficient of 0.123 $cm^{-1}$ was used in all calculations.

### 4.3 Determination of ABF and TBF

The extracted liver TAC was split into its two components (arterial and portal) using the constrained deconvolution technique described briefly above (**11**). The input curve used was the lung TAC. Absolute hepatic arterial flow was calculated according to equation (3), with $C_B$ determined as described above. It should be noted that if the liver curve is extracted using data from only a portion of the organ its magnitude is representative only of flow to this region. ABF must therefore be appropriately scaled to correct for this and hence determine total arterial flow. Scaling is achieved by multiplying the result of equation (3) by the quotient $C_{full}/C_{partial}$, where $C_{full}$ represents the total count rate from the liver in the anterior colloid image and $C_{partial}$ represents the count rate on the same image from the region over the liver used for the extraction of the liver curve. No image alignment was necessary since the patient was not moved between the colloid and the HSA studies. TBF was simply determined by dividing the total arterial flow by the arterial fraction [equation (4)]. Portal vein flow (PVF) was obtained as a by-product from the difference between the total (TBF) and the arterial flows.

Reproducibility of data analysis techniques was assessed by reprocessing of the data ($n = 6$) by a single observer.

## 5 RESULTS

Typical TACs for a volunteer and a cirrhotic subject are given in Figs 1 and 2 respectively. The reconstructed liver curves for the data given in Figs 1 and 2, obtained by reconvolution of the impulse retention function with the lung TAC, are compared with the actual liver curves, together with the hepatic arterial and portal venous contributions to these curves.

Table 1 gives details of individual patient results. Reprocessing of the data gave the following coefficients of variation for the four parameters: AF 4.4 per cent, ABF 10.6 per cent, PVF 6 per cent, TBF 7.1 per cent.

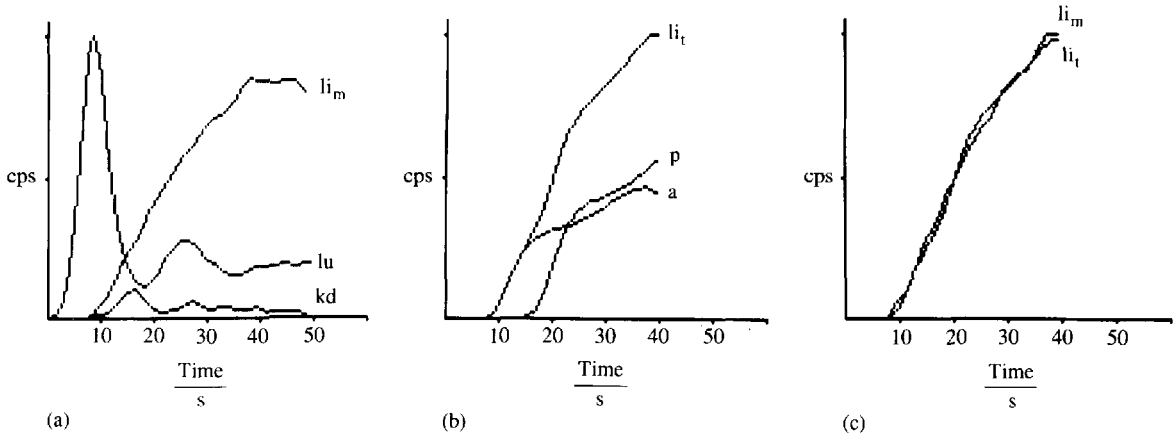


**Fig. 1** (a) TACs for liver ($li_m$), lung (lu) and kidney (kd) for a volunteer subject (the kidney curve arises as a by-product of the factor analysis technique and is used for removal of cross-talk)
(b) Reconstructed liver curve ($li_t$) obtained by the reconvolution of the impulse retention function with the lung TAC. a and p represent the hepatic arterial and portal contributions to $li_t$
(c) Comparison of liver TAC and reconstructed curve

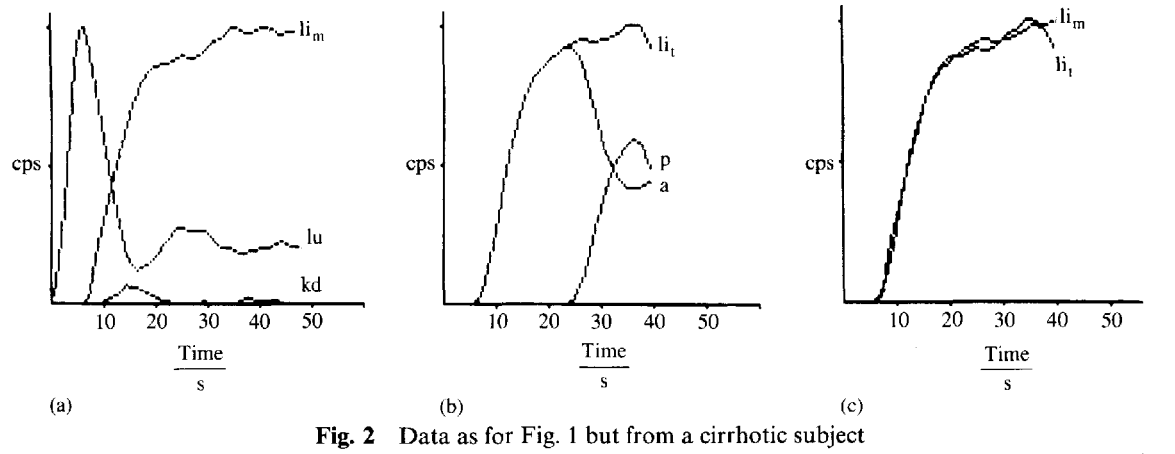


**Fig. 2** Data as for Fig. 1 but from a cirrhotic subject

## 6 DISCUSSION

The results of this preliminary study suggest that it may be possible to obtain an absolute measure of total liver blood flow using non-invasive radioisotope techniques. While validation of the method by comparison with standard more-invasive techniques for measuring liver blood flow is obviously necessary, the close agreement between the values for TBF and AF for non-cirrhotic and volunteer subjects and currently accepted normal values for these parameters (**15**, **16**) is encouraging.

The coefficients of variation obtained by repeat processing of the data are relatively low, despite the complexity of the analysis procedure. This probably reflects the attention that has been given to automating the processing technique where possible to minimize operator intervention. The error in TBF is of the order of 7–8 per cent; further work to assess reproducibility of the overall technique by repeat isotope administrations is in progress.

It is pertinent at this point to consider some of the assumptions and potential errors involved in this technique. The method assumes that the lung TAC is an accurate representation of the temporal variation in blood concentration in the hepatic artery. Thus, integration of this curve, with appropriate scaling, should yield the hypothetical liver curve that would arise under conditions of complete tracer extraction and zero portal flow. The true arterial curve will be the convolution of the lung curve and the distribution of transit times between the lung and the arterial input to the liver. If the transit time spectrum is narrow the lung curve will be a good representation of the input to the liver. As bolus smearing becomes more pronounced, the deviation between the curves will become greater, leading to an underestimation of hepatic artery flow. A visual comparison of the width of velocity waveforms between the ascending aorta and the middle abdominal aorta in a canine model (**17**) suggests that bolus smearing between these sites is minimal. Most of the bolus spreading that occurs between the antecubital vein and the hepatic artery occurs in the pulmonary vascular bed (**18**). The use of a lung curve as input will take this into account. Furthermore, given the difficulty of extracting uncontaminated arterial TACs from the abdominal region, the lung curve is likely to provide the best estimate of blood concentration for the present study.

The effect of background activity is not considered in the analysis. While background is generally considered to be of negligible importance in first-pass studies, the late arrival of tracer in the liver from the portal vein may coincide with or follow tracer delivery to the superficial tissues from their arterial supply. The effect of this would be to contaminate the portal component of the

**Table 1** Patient results

| Patient | Classification* | TBF ml/min | AF | ABF ml/min | PVF ml/min |
|---|---|---|---|---|---|
| 1 | C | 2122 | 0.57 | 1200 | 922 |
| 2 | C | 4596 | 0.63 | 2883 | 1686 |
| 3 | C | 4256 | 0.52 | 2226 | 2031 |
| 4 | C | 4347 | 0.58 | 2535 | 1812 |
| 5 | C | 1484 | 0.55 | 818 | 665 |
| 6 | C | 1521 | 0.47 | 720 | 801 |
| 7 | C | 1438 | 0.50 | 723 | 715 |
| 8 | C | 1851 | 0.59 | 1087 | 764 |
| 9† | NC | 1615 | 0.39 | 633 | 982 |
| 10† | NC | 951 | 0.29 | 275 | 676 |
| 11 | NC | 1460 | 0.49 | 717 | 743 |
| 12† | NC | 682 | 0.35 | 236 | 446 |
| 13 | NC | 1488 | 0.35 | 525 | 936 |
| 14† | NC | 1467 | 0.33 | 485 | 982 |
| 15 | NC | 1058 | 0.47 | 495 | 563 |
| 16‡ | NC | 1285 | 0.21 | 272 | 1013 |
| 17‡ | NC | 954 | 0.34 | 321 | 663 |
| Cirrhotics | | | | | |
| Median | | 1987 | 0.56 | 1144 | 862 |
| Range | | 3158 | 0.16 | 2163 | 1366 |
| Non-cirrhotics | | | | | |
| Median | | 1285 | 0.35 | 485 | 743 |
| Range | | 933 | 0.28 | 481 | 567 |

* C = cirrhotic, NC = non-cirrhotic.
† Non-cirrhotic subjects with alcoholic liver injury of fat minor fibrosis.
‡ Volunteer subjects.

liver signal with a background contribution. Under these conditions, AF will be underestimated and TBF overestimated. It can be shown that the magnitude of these errors will be dependent on the size of the background signal relative to the sum of the arterial and portal flows.

A further problem arises in relation to the background activity in the determination of the calibration factor $C_c$. While the background contribution is negligible in the first-pass lung TAC, this is less likely to be true when the HSA tracer has attained equilibrium, that is at the time the blood sample is taken. The effect of such background contamination would be to raise the value of $H(t)$ in equation (5), thus increasing the calculated values of ABF and TBF.

The height of the portal component of the IRF is only representative of portal flow if the minimum intrahepatic intravascular transit time is greater than the spectrum of transit times through the portal bed. If this condition is not met, portal flow will be underestimated.

Errors may arise in the measurement of absolute activity in the liver, as determined from the colloid images. This measurement is necessary for the calculation of the attenuation correction factor, $C_B$; the errors associated with it have been discussed elsewhere (**14**).

The development of extrahepatic and intrahepatic shunts is a characteristic feature of liver disease. Intrahepatic shunting of blood may be regarded as 'non-functional' flow, since the blood does not come into contact with the hepatocyte mass. The method of measuring hepatic blood flow described in the present study uses a non-extracted tracer and will not distinguish between functional and non-functional flows. The TBF determined thus represents the sum of the blood flowing through the sinusoids and that flowing through intrahepatic shunts.

The simplifying assumptions that form the core of this model are based on normal rather than pathological conditions. The method assumes that there are always two components of hepatic flow, which are temporally separated on the first pass. This constraint may lead to instabilities in the presence of complete portocaval shunting, since if only one component is present this may effectively be partitioned into two equal components. Further sophistication of the technique is therefore required in such circumstances. Notwithstanding this, the close agreement between the results obtained in the non-cirrhotic and volunteer subjects and published normal values is encouraging and suggests that the technique may prove useful in the study of liver physiology and the effects of therapeutic intervention.

## REFERENCES


1 **Bradley, S. E., Ingelfinger, F. J., Bradley, G. P.,** *et al.* The estimation of hepatic blood flow in man. *J. Clin. Invest.*, 1945, **24**, 890–897.
2 **Caesar, J., Shaldon, S., Chiandussi, L.,** *et al.* The use of indocyanine green in the measurement of hepatic blood flow and as a test of hepatic function. *Clin. Sci.*, 1961, **21**, 43–57.
3 **Hirsch, L. J.** and **Rone, A. S.** Hepatic arterial and portal flow in cardiogenic and hemorrhagic shock in awake dogs. *Circ. Shock*, 1982, **9**, 17–26.
4 **Wilkinson, G. R.** and **Shand, D.** A physiological approach to hepatic drug clearance. *Clin. Pharmacol. and Therapeutics*, 1975, **187**, 377–390.
5 **Bru, C., Bosch, J., Navassa, M.,** *et al.* Pulsed-Doppler measurements of portal blood flow in cirrhosis: applications in the non-invasive evaluation of pharmacological therapy of portal hypertension. *J. Hepatol.*, 1986, **3** (Suppl. 1), S24.
6 **Miller, J., Diffey, B. L.** and **Fleming, J. S.** Measurement of colloid clearance rate as an adjunct to static liver imaging. *Eur. J. Nucl. Med.*, 1979, **4**, 1–5.
7 **Groszman, R. J.** The measurement of liver blood flow using clearance technique. *Hepatology*, 1983, **3**, 1039–1040.
8 **Brown, P. H., Juni, J. E., Leiberman, D. A.,** *et al.* Hepatocyte versus biliary disease: a distinction by deconvolutional analysis of technetium-99m IDA time-activity curves. *J. Nucl. Med.*, 1988, **29**, 623–630.
9 **Magrini, A., Izzo, G., Guerrisi, M.,** *et al.* A new approach to non-invasive quantitative study of hepatic haemodynamics using radioactive colloids *in vivo*. *Clin. Phys. Physiol. Measmt*, 1985, **6**, 179–204.
10 **Peters, A. M., Gunasekera, R. D., Henderson, B. L.,** *et al.* Non-invasive measurement of blood flow and extraction fraction. *Nucl. Med. Commun.*, 1987, **8**, 823–837.
11 **Barber, D. C.** and **Tindale, W. B.** Determination of the arterial flow fraction in normal and diseased livers using constrained deconvolution. *Proc. Instn Mech. Engrs*, Part H, 1992, **206** (H2), 93–98.
12 **Juni, J. E., Merion, R. M., Campbell, D. A.,** *et al.* Diagnosis of liver transplant rejection by scintigraphy with deconvolutional analysis. *J. Nucl. Med.*, 1988, **29**, 790.
13 **Martel, A.** and **Barber, D. C.** A new approach to dynamic study analysis. In *Information processing in medical imaging* (Eds A. Ortendahl and J. Llacer), 1991, pp. 327–340 (Wiley–Liss, New York).
14 **Fleming, J. S.** A technique for the absolute measurement of activity using a gamma camera and computer. *Phys. Med. Biol.*, 1979, **24**, 176–180.
15 **Bell, G. H., Davidson, J. N.** and **Emslie-Smith, D.** *Textbook of physiology and biochemistry*, 1972, p. 584 (Churchill-Livingstone, London).
16 **Berne, R. M.** and **Levy, M. N.** *Cardiovascular physiology*, 1986, p. 228 (C. V. Mosby Company, St Louis, Miss.).
17 **Caro, C. G., Pedley, J. J., Schroter, R. C.,** *et al.* *The mechanics of the circulation*, 1978, p. 271 (Oxford University Press, Oxford).
18 **Peters, A. M., Brown, J., Crossman, D.,** *et al.* Noninvasive measurement of renal blood flow with technetium-99m-DTPA in the evaluation of patients with suspected renovascular hypertension. *J. Nucl. Med.*, **31**, 1980–1985.